

NDVI Threshold Classification for Detecting Vegetation Cover in Damietta Governorate, EgyptM. I. El-Gammal¹, R. R. Ali² and R. M. Abou Samra¹¹Environmental Science Department, Faculty of Science, Damietta University, Egypt²Soils and Water Use Department, National Research Centre, Cairo, Egyptrasha.mohamed67@yahoo.com

Abstract: The aim of this study is to detect vegetation cover change at Damietta governorate by using remote sensing technique. To fulfill this objective, three Landsat images (path 176, row 038) acquired in 1987 (TM), 2004 (ETM+) and 2013 (Landsat-8) were used to map the land cover and monitor NDVI over the investigated area. The threshold NDVI classification analysis revealed three vegetation cover groups including no plant cover, weak plants and healthy plants, which were designated in an increasing order of vegetation vigor. Vegetation cover revealed significant spatial and temporal changes. There was a general decrease in vegetation cover indicating a trend of degradation of the ecosystem. The spatial pattern in the classified images showed that the "healthy plants" had decreased in the 1987-2013 period, by 19.1% and by 10.1% in the 2004- 2013 period.

[M. I. El-Gammal, R. R. Ali and R. M. Abou Samra. **NDVI Threshold Classification for Detecting Vegetation Cover in Damietta Governorate, Egypt.** *J Am Sci* 2014;10(8):108-113]. (ISSN: 1545-1003). <http://www.jofamericanscience.org>. 15

Keywords: NDVI, remote sensing, land cover, Damietta Governorate, Egypt

1. Introduction

Human activities affect the dynamics of ecosystems (especially natural vegetation cover) and other earth systems. For instance, the modification of vegetation cover, with a predominant clearing of natural vegetation may have long term impact on sustainable food production, freshwater and forest resources, the climate and human welfare (**Badamasi and Yelwa, 2010**). Various remote-sensing-based studies have revealed compelling spectral relationships between the red and near-infrared (NIR) part of the spectrum to green vegetation. Due to vegetation pigment absorption (chlorophyll, protochlorophyll), the reflected red energy decreases, while the reflected NIR energy increases as a result of the strong scattering processes of healthy leaves within the canopy. Directly using the amount of reflected red and/or NIR radiation to study the biophysical characteristics of vegetation is very inadequate for reasons rooted in the intricate radiative energy interaction at the canopy level, background, and atmospheric impacts on the signal and the non-uniqueness of the signatures. However, when two or more bands are combined into vegetation index (VI), the vegetation signal is boosted and the information becomes more useful. Vegetation indices can then be used as surrogate measures of vegetation activity (**Brown et al., 2006**).

Vegetation indices are based on the characteristic reflection of plant leaves in the visible and near-infrared portions of light. Healthy vegetation has low reflection of visible light (from 0.4 to 0.7 μm), since it is strongly absorbed by leaf pigments (chlorophyll) for photosynthesis. At the same time, there is high

reflection of near-infrared light (from 0.7 to 1.1 μm). The portion of reflected near-infrared light depends on the cell structure of the leaf. In fading or unhealthy leaves, photosynthesis decreases and cell structure collapses resulting in an increase of reflected visible light and a decrease of reflected near infrared light (**Gross, 2005**).

NDVIs properties help mitigate a large part of the variations that result from the overall remote-sensing system (radiometric, spectral, calibration, noise, viewing geometry, and changing atmospheric conditions). Some land-surface types are not robustly represented by NDVI, such as snow, ice, and non-vegetated surfaces, where atmospheric variations and sensor characteristics dominate (**Brown et al., 2006**). The resolution of satellite-borne remotely sensed imagery is such that picture elements (pixels) commonly represent multiple land covers. In addition, remote sensing instruments sense electromagnetic energy that has travelled through the atmosphere. Thus, the seasonal character of vegetation index measurements over time may exhibit trends that represent changes in land cover and viewing conditions (such as changes in the presence of water vapor and aerosols) as well as true phenological responses. Consequently, it is more accurate to state that such studies are concerned with trends in the seasonality of NDVI. NDVI has been shown to be very sensitive to ecosystem conditions, particularly when paired with maximum value compositing to reduce the effects of atmospheric contaminants, such as clouds and aerosols. Therefore it is of considerable value as an indicator of environmental change (**Eastman et al., 2013**).

Among the various remote sensing-based vegetation measures utilized in agricultural monitoring, Normalized Difference Vegetation Index (NDVI) is the most widely used proxy for vegetation cover and production. Therefore, there is a strong relationship between NDVI and agricultural yield. Vegetation properties, such as length of growing season, onset date of greenness, and date of maximum photosynthetic activity are often derived from NDVI time series for monitoring changes in agricultural systems. These phenological indicators emphasize different characteristics of terrestrial ecosystems to gain a better understanding of structure and function of land cover and associated changes. Phenology, the timing of recurring life cycle events, may for example shift in response to natural or anthropogenic disturbances in agricultural ecosystems (Yin et al., 2012).

Different ecosystem changes can be analyzed from NDVI time series, for example, annual mean or peak NDVI provides an integrated view on photosynthetic activity. The seasonal NDVI amplitude is related to the composition of evergreen and deciduous vegetation and the length of the NDVI growing season can be related to phenological changes. Thus, trend detection in NDVI time series can help to identify and quantify recent changes in ecosystem properties from a local to global scale (Forkel et al., 2013).

Remote sensing (RS) techniques have been identified to provide a viable source of data from which updated land cover information can be extracted efficiently in order to monitor ecosystem changes. Vegetation cover is an obvious part of land cover. Land cover undergoes changes due to natural or man-made causes over time. Change detection has become a major application of remotely sensed data because of repetitive coverage at short intervals and consistent image quality. Change detection is the process of identifying differences in the state of an object or phenomenon by observing it at different times. This involves the use of multi-temporal satellite data sets to discriminate areas of land cover change between dates of imaging and involve data acquired by the sensors having same (or similar) characteristics. The basic premise in using remote sensing data for change detection is that changes in land cover result in changes in radiance values and changes in radiance due to land cover change are large with respect to radiance change caused by others factors such as differences in atmospheric conditions, differences in soil moisture and differences in sun angles. Changes in vegetation reflectance are a useful basis to judge the relative success of protected area management. Hence, vegetation cover managed in time one can be compared to vegetal cover managed at different time,

after adjusting for unplanned or uncontrollable variations (Badamasi and Yelwa, 2010).

2. Materials and Methods

The Study Area

Damietta governorate is located at the northeast of the Nile Delta between longitudes 31° 28' & 32° 04' and latitude 31° 10' & 31° 30' (Fig. 1). The governorate covers an area of 227575.32 acres, representing 0.1% of the Republic's area, and encompasses 4 districts, 10 cities, 47 rural units and 85 villages. According to the preliminary results of 2006 census, population is about 1.1 million people; 38.4% of them live in urban areas and 61.6% in rural areas. The population natural growth rate is 21.6 per thousand. The governorate cultivated area covers 108.8 thousand acres and is famous for growing wheat, maize, cotton, rice, potatoes, lemons, grapes, and tomatoes (CAPMAS, 2011).

Damietta Governorate's Mediterranean coastline extends for some 61 km from El-Diba in the east to Gamasa in the west. The governorate encompasses 4 marakz and 11 cities (SEAM, 2005). The Damietta promontory was formed by sediment transported to the coast through Damietta river during Holocene transgression (El Askary and Frihy, 1986; Countellier and Stanley, 1987). The Damietta branch is one of the two major distributaries of the River Nile. The largest resort community of Ras El Bar is located west of the river. Manzala lagoon, the largest of the Nile delta lagoons, is about 50 km in length with a maximum width of 22 km. El Gamil inlet connects the lagoon to the sea. The lagoon is shallow depth up to 1.7 m, water is brackish with fresh water discharging mainly from canals and drains located along the southern and western borders of the lagoon. Numerous chains of islands of varying size are scattered throughout the lagoon, having a maximum length of 18 km. These islands could be remnants of older coastal features, like beach ridges, dunes and riverbanks (CRI/UNESO/UNDP, 1978). The south and southeastern margins of Manzala lagoon have extensive areas of marshes and swamps. At the western part of Damietta river branch there is the Damietta harbor, which considered a very important for wood industry.

The area is characterizes by a climate of Mediterranean Sea with hot arid summer and moderate rain winter. The mean temperatures are especially high in the dry season where they range between 25°C and 30 °C with average temperature of 22°C and the difference between the average temperature in summer and winter is 6°C representing thermal temperature range (Climatological Normal for Egypt, 2011). In the summer, Mediterranean Sea air blows reducing the temperature, while in the

winter the western wind blows on the north of the Delta carrying rainy clouds and passes over the coast resulting in rainfall on the Delta. Moreover, spring months characterized by blowing the "Khamasin" dust laden winds, which is hot, dry, and dust-laden winds and are mainly southern and eastern winds, occur frequently during the period of February to June.

Remote Sensing Data

Three Landsat images (path 176, row 038) acquired in 1987 (TM), 2004 (ETM+) and 2013 (Landsat-8) were used in this study to obtain land cover and monitor NDVI over the investigated area (**Table 1**).

Digital Image Processing

Images were radiometrically and geometrically corrected to accurate the irregular sensor response over the image and to correct the geometric distortion due to Earth's rotation (**ITT, 2009**). Specification of Landsat-7 ETM+ and Landsat-8 are illustrated in **Table 2**.

Data Analysis

Land Cover Map

Land use/land cover map was prepared using knowledge-based supervised classification. Identifying known a priori through a combination of fieldwork, map analysis, and personal experience as training sites; the spectral characteristics of these sites have used to train the classification algorithm for eventual land-cover mapping of the remainder of the image. Each pixel both within and outside the training sites is then evaluated and assigned to the class of which it has the highest likelihood to be a member. The imagery was visually interpreted to prepare land use/land cover map using knowledge-based supervised classification in ENVI 5 Imagine. The output of the supervised classification was divided into 8 land cover classes.

Calculating NDVI

Prior to image classification, a Normalized Difference vegetation Index (NDVI) images were generated. A simple classification technique was then applied to the NDVI images of 1987, 2004 and 2013 using ENVI 5 and Arc-GIS 10.2 software. NDVI images are obtained by calculating the ratio between the visible (VIS) and near-infrared (NIR) bands of the satellite image. This emphasizes the characteristics and the different statuses of plant vigor and density even further. Mathematically written, the equation is as follows:

$$NDVI = (NIR - VIS) / (NIR + VIS)$$

NDVI values are always in between -1 and +1, where higher values represent more vigorous and healthy vegetation. According to **Gross (2005)**, very low values (0.1 and lower) correspond to barren areas of rock, sand and snow. Moderate values (0.2 to 0.3) indicate shrub and grassland, while temperate and

tropical rainforests are represented by high NDVI values (0.6 to 0.8).

Change Rate Analysis

Change rates in vegetation cover type were analyzed using the following formulae (**Badamasi and Yelwa, 2010**):

- i. Change area = $D2 - D1$, where D1 and D2 are the area of the target vegetation cover type at the beginning (1987) and the end (2013) of the study period, respectively.
- ii. % change = $(\text{change area} / A) \times 100$, where A is the total area.
- iii. Annual rate of change (km^2/year) = $(\text{change area} / T_i)$, where T_i is number of years between the beginning and the end of study period.
- iv. % annual rate of change ($\%/ \text{year}$) = $\text{change area} / (D1 \times T_i)$

3. Results and Discussion

Land Cover Map

Land use/land cover map and use/land cover map as represented in **Fig. 2** was prepared using knowledge-based supervised classification. The areal extent of land-cover classes is given in **Table 3**. The results revealed that cultivation with an area of 349.49 km^2 is a predominant land-cover class, accounting for 38.8% of the entire study area. About 4.8 % of the area is covered by native vegetation and fallow fields occupy 13.2% of the total area. The sand cover account for an area of about 3.6%. Urban is a vital land-use class and holds about 17.6% of the total area. Water bodies occupy 16 % of the total area. Salt marsh represents 0.4% of the total area.

NDVI

NDVI values were calculated (**Fig. 3a, b and c**). Then, the values were reclassified into three groups; these included "no plant cover, weak plants and healthy plants" which were designated in an increasing order of vegetation vigor. **Table 4** shows the threshold and the distribution of vegetation cover classes across the different images. The vegetation classification maps clearly illustrated the spatial patterns of vegetation cover distribution in the governorate (**Fig. 4 a, b, and c**). The classified image of 1987 showed that the vegetation cover is dominated by "healthy plants" accounting for more than 57.6%, followed by "weak plants", accounting for about 25.4%. No plant cover account for 17 %. The spatial pattern in the classified 2004 image showed "healthy plants" accounting for about 48.6% of the areal coverage as against the earlier coverage of 57.6% in 1987. In addition, the "weak plants" and "no plant cover" had increased by 6.1% and 2.9%, respectively within the same period. However, the spatial pattern was entirely different in the classified 2013 image, which showed both "weak plants" and "no plant

cover" cumulatively accounting for about 61.5% of the areal coverage. In addition, the "healthy plants" had decreased by 19.1% and 10.1% than in 1987 and 2004, respectively (Fig. 5).

Change Rate

Table 5 shows the changed area and the rate of change between 1987 and 2013. As revealed from the results, there were variability in the percent and

annual rate of change between the different vegetation classes. "No plant cover" and "weak plants" increased at a rate of 3.58 km²/year (3.14% / year) and 1.36 km²/year (0.8% / year), respectively over a period of 26 years (i.e. 1987-2013). The "healthy plants" decreased at a rate of 4.94 km²/ year (1.28% / year). It is clear that the vegetation vigour was declining.

Table 1: Remotely sensed data used for the study

Images Used for the study	Path/row	Resolution	Date of acquisition
Landsat 5 TM	176/38	30m	22-4-1987
Landsat 7 ETM+	176/38	30m	12-4-2004
Landsat-8	176/38	30m	29-4-2013

Note: TM = thematic mapper; ETM+ = enhanced thematic mapper plus

Table 2: Comparison of Landsat-7 ETM+ and Landsat-8 OLI/thermal infrared sensor (TIRS) spectral bands (Li et al., 2014)

Landsat-8 OLI and TIRS		Landsat-7 ETM+		Spatial Resolution (m)
Bands	Wavelength (µm)	Bands	Wavelength (µm)	
Band 1—Coastal aerosol	0.43–0.45	NA	--	30
Band 2—Blue	0.45–0.51	Band 1	0.45–0.52	30
Band 3—Green	0.53–0.59	Band 2	0.52–0.60	30
Band 4—Red	0.64–0.67	Band 3	0.63–0.69	30
Band 5—Near infrared (NIR)	0.85–0.88	Band 4	0.77–0.90	30
Band 6—Short-wave infrared (SWIR 1)	1.57–1.65	Band 5	1.55–1.75	30
Band 7—Short-wave infrared (SWIR 2)	2.11–2.29	Band 7	1.55–1.75	30
Band 8—Panchromatic	0.50–0.68	Band 8	0.52–0.90	15
Band 9—Cirrus	1.36–1.38	NA	--	30
Band 10—Thermal infrared (TIRS) 1	10.60–11.19	Band 6	10.40–12.50	TIRS/ETM+: 100/60 * (30)
Band 11—Thermal infrared (TIRS) 2	11.50–12.51			

* ETM+ band 6 and TIRS thermal bands are acquired at the resolution of 60 and 100 meters, respectively, but all are resampled to 30-meter pixels in the delivered data product. The above information was compiled from the USGS Landsat Missions webpage (http://landsat.usgs.gov/band_designations_landsat_satellites.php).

Table 3: Areal extent of the land cover classified from Landsat-8 image of the governorate acquired in 2013

Land cover	Area (km ²)	Percentage %
Native vegetation	43.94	4.8
Cultivation	349.49	38.8
Fallow fields	120.16	13.2
Fish ponds	51.22	5.6
Salt marsh	3.67	0.40
Sand	33.50	3.6
Urban	159.72	17.6
Water bodies	145.18	16
Total	906.91	100

Table 4: Class covers distribution classified by thresholds

Class cover	Thresholds (NDVI values)			1987		2004		2013	
	1987	2004	2013	Area (Km ²)	(%)	Area (Km ²)	(%)	Area (Km ²)	(%)
No plant cover	[-0.50 - 0]	[-0.52 - 0]	[-0.38 - 0]	114	17	154.6	23.1	207	30.9
Weak plants	[0.01-0.3]	[0.01-0.3]	[0.01-0.3]	170	25.4	189.9	28.3	205.4	30.6
Healthy plants	[0.31- 0.77]	[0.31- 0.72]	[0.31- 0.61]	386.5	57.6	326	48.6	258.1	38.5
Total Area				670.5	100	670.5	100	670.5	100

Table 5: Area and rate of change between 1987 and 2013

Type of cover	Change area (km ²)	% change	Annual rate of change (km ² /year)	% Annual rate of change (%/year)
No plant cover	93	13.87	3.58	3.14
Weak plants	35.4	5.28	1.36	0.8
Healthy plants	-128.4	-19.15	-4.94	-1.28

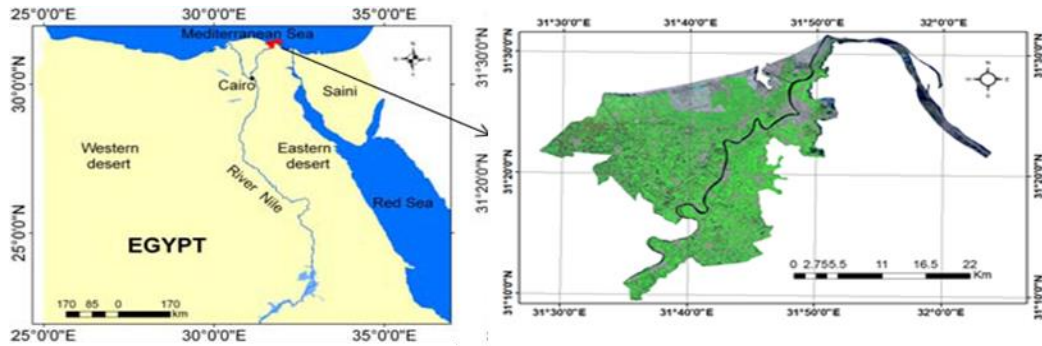


Fig. 1: Location of Damietta governorate on Egypt map (to the left) and Landsat-8 image of the governorate acquired in 2013 (to the right).

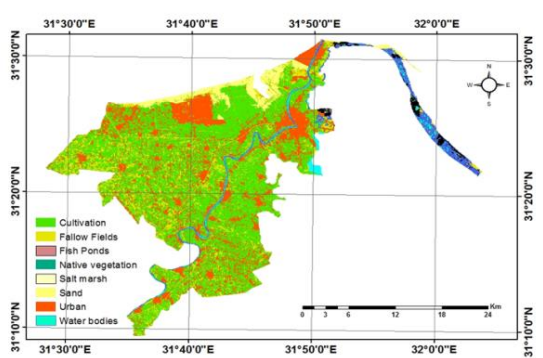


Fig. 2: Land -cover map as extracted from supervised classification of 2013 Landsat-8 Image

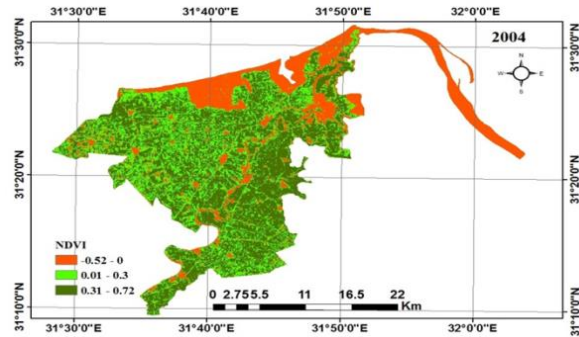


Fig. 3b: NDVI values of 2004

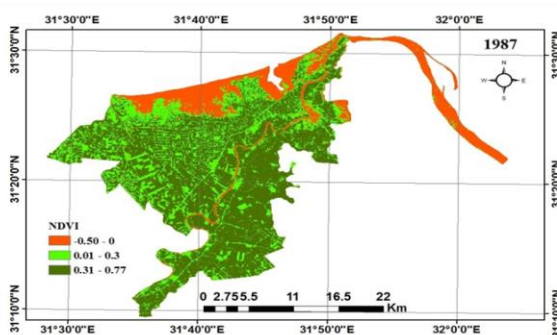


Fig. 3a: NDVI values of 1987

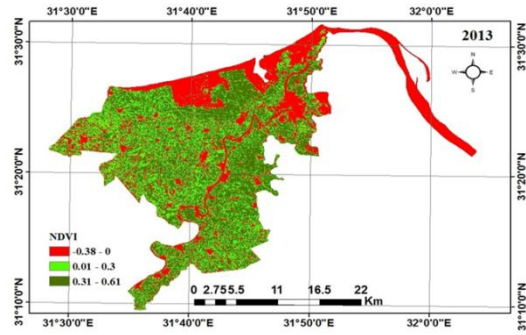


Fig. 3c: NDVI values of 2013

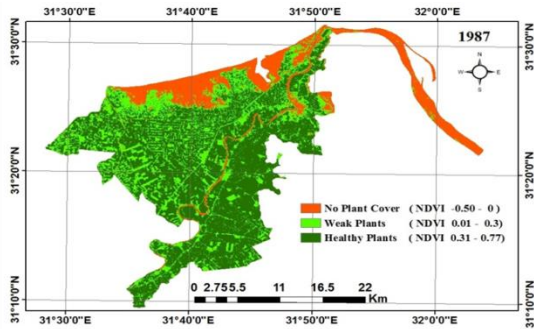


Fig. 4a: Plant status and NDVI values in 1987

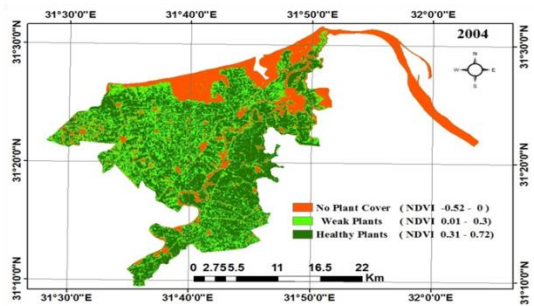


Fig. 4b: Plant status and NDVI values in 2004

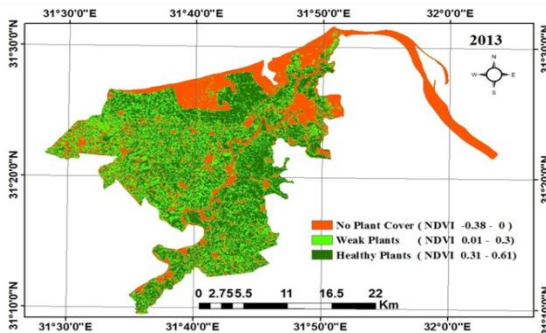


Fig. 4c: Plant status and NDVI values in 2013

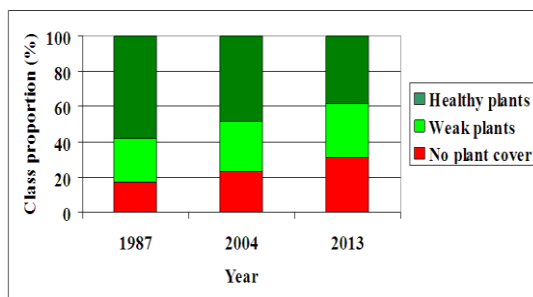


Fig. 5: Percentage proportions of vegetation cover classes from 1987 to 2013 years

Conclusion

In this study, remote sensing used to investigate the changes of vegetation cover in Damietta Governorate. Three Landsat images acquired on 1987,

2004 and 2013 were used. There were variability in the percent cover change and annual rate of change between the different cover classes. The "No plant cover" and "weak plants" classes were increased at a rate of 3.14% and 1.36 0.8% per year, respectively over a period of 26 years (i.e. 1987-2013). On the other hand "healthy plants" decreased at a rate of 1.28% per year-during the same period.

References

- Badamasi, M. M. and Yelwa, S. A. (2010).** Change detection and classification of land cover at Falgore game reserve: A Preliminary assessment. *BEST Journal*. 7 (1): 75-83.
- Brown, M. E., Pinzon, J.E.; Didan, K.; Morisette, J.T.; Tucker, C.J. (2006).** "Evaluation of the consistency of long-term NDVI time series derived from AVHRR, SPOT-Vegetation, SeaWiFS, MODIS, and Landsat ETM+ sensors." *Geoscience and Remote Sensing, IEEE Transactions on* 44(7): 1787-1793.
- CAPMAS, (2011).** Mobilization and Statistic of Damietta Governorate. Central Agency for Public Mobilization and Statistics (CAPMAS) **Cairo, Egypt.**
- Climatological Normal for Egypt (2011).** The normal for Damietta Governorate from 1960 to 2011, Ministry of Civil Aviation, Meteorological Authority, Cairo, Egypt.
- Countellier, V. and Stanley, J. (1987).** Late Quaternary Stratigraphy and Paleogeography of the Western Nile Delta, Egypt, *Marine Geol.*; 257-275.
- CRI/UNESO/UNDP (1978).** Coastal Protection Studies, Final Technical Report, Paris, 1, 155 p.
- Eastman, J. R.; Sangermano, F.; Machado, E. A.; Rogan, J. and Anyamba, A. (2013).** "Global trends in seasonality of normalized difference vegetation index (NDVI), 1982–2011." *Remote Sensing* 5(10): 4799-4818.
- El Askary, M.A. and Frihy, O.E. (1986).** Depositional Phases of Rosetta and Promontories on the Nile Delta Coast, *J. Afr. Earth Sci.*; 627-633.
- Forkel, M., N. Carvalhais, Verbesselt, J., Mahecha, M.D; Neigh, Ch. and Reichstein, M. (2013).** "Trend change detection in NDVI time series: effects of inter-annual variability and methodology." *Remote Sensing* 5(5): 2113-2144
- Gross, D. (2005).** Monitoring Agricultural Biomass Using NDVI Time Series, Food and Agriculture Organization of the United Nations (FAO), Rome, Italy.
- ITT, (2009).** ITT Corporation ENVI 4.7 Software, 1133 Westchester Avenue, White Plains, NY 10604, USA.

Li, P.; Jiang, L. and Feng, Z. (2014). Cross-Comparison of Vegetation Indices Derived from Landsat-7 Enhanced Thematic Mapper plus (ETM+) and Landsat-8 Operational Land Imager (OLI) Sensors. *Remote Sens*, 6, 310-329

SEAM (2005). The Support for Environmental Assessment and Management Programme, Damietta Governorate Environmental Action Plan, UK Department of International Development, Egyptian Environmental Affairs Agency, p.9-72.

Yin, H.; Udelhoven, T.; Fensholt, R.; Pflugmacher, D.; and Hostert, P. (2012). How Normalized Difference Vegetation Index (Ndvi) Trends from Advanced Very High Resolution Radiometer (AVHRR) and Système Probatoire D'observation De La Terre Vegetation (Spot Vgt) Time Series Differ In Agricultural Areas: An Inner Mongolian Case Study, *Remote Sens.*, 4(11): 3364-3389.

7/5/2014